Research Article

Wentao Hu and Tandong Yao*

Geometric similarity of the twin collapsed glaciers in the west Tibet

https://doi.org/10.1515/geo-2020-0316
received March 10, 2021; accepted November 04, 2021

Abstract: Two adjacent glaciers collapsed consecutively in the Western Xizang Autonomous Region, China, on July 17 and September 21, 2016, presumably triggered by relatively intensive climate change in this region, leading to massive downstream ice and mud avalanches. After these twin glacier collapses, there have been many researches, which mainly focus on the physical characteristics of these two glaciers while lack the differences between them and the other glaciers. In this study, the geometric features and energy distribution along the glacier centerlines are investigated to identify the differences between these two collapsed glaciers and other glaciers in the western Tibetan Plateau. The anomaly of climate change is presumed to be the trigger of the twin glacier collapses in accordance with existing research results, whereas in this study, the striking geometric similarity between the centerlines of the twin glaciers, which is quantitatively interpreted by the Fréchet distance among the glacier centerlines, unearth some novel mechanisms. The essential point in these new mechanisms is the energy distribution along the glacier centerlines. A hypothesis based on the principle of energy conservation is derived to demonstrate the mechanisms and dynamic processes of the glacier collapses. Furthermore, on the basis of the geometric similarity and energy distribution of the glacier centerlines, a risk assessment of glacier collapse in the western Tibetan Plateau is implemented to facilitate glacier disaster prevention.

Keywords: glacier collapses, OGGM, geometric similarity, Fréchet distance, western Tibetan Plateau, glacier centerlines

*** Corresponding author: Tandong Yao,** Institute of Tibetan Plateau Research, Chinese Academy of Sciences, 100101, Beijing, China, e-mail: tdyao@itpcas.ac.cn
Wentao Hu: Institute of Tibetan Plateau Research, Chinese Academy of Sciences, 100101, Beijing, China; College of Resources and Environment, University of Chinese Academy of Sciences, 100101, Beijing, China, e-mail: hwt11@itpcas.ac.cn, tel +86-185-1543-8847
ORCID: Wentao Hu 0000-0003-2117-5873

1 Introduction

The western Tibetan Plateau (longitude 79° to 92°E, latitude 28° to 37°N, mean elevation >5,000 m above sea level, Figure 1) is located in the rain shadow of three high strongly glacierized mountain ranges [1]. In the Randolph Glacier Inventory (RGI 6.0), it is reported that approximately 20,000 glaciers are widely distributed in this region, and the downstream glacier-fed rivers and lakes provide water resources to local nomadic herders and their yaks [2]. Therefore, the solid water resources including the ice and snow cover in the glacierized western Tibetan Plateau are of significance to the surrounding countries and regions [3].

However, the solid water resources had sustained a great loss in 2016. Within 3 months in that year, two adjacent glaciers (Aru-1 and Aru-2) collapsed, consecutively, on July 17 and September 21, 2016 in the western Tibetan Plateau (Figure 2), receiving considerable attention from the scientific community [4]. In these twin catastrophes, nearly the whole glaciers flowed downward into the alluvial areas below the glacier valleys, with two estimated source volumes of approximately 70 and 100 Mm^3, which destroyed pastures and buried nine habitants and hundreds of livestock [5]. Furthermore, the massive loss of valuable solid water resources in this considerably dry region has a negative environmental impact on the local fragile ecosystem [6].

When and where the next one of this kind of catastrophe would take place have left cryospheric scientists puzzled [7]. Even though anomalous glacier movements are not rare in the western Tibetan Plateau [8], such sudden massive glacier collapses have not been historically recorded [9]. Many researchers have investigated the magnitude, mechanisms, and subsequent impacts of the twin glacier collapses. One study provided an overview of the two glaciers and the twin collapses [5]. These two glaciers are not temperate but cold based and frozen to the bed, which are rather dynamically stable in the past decades. On the basis of their field investigation and the local meteorological data, the rising temperature

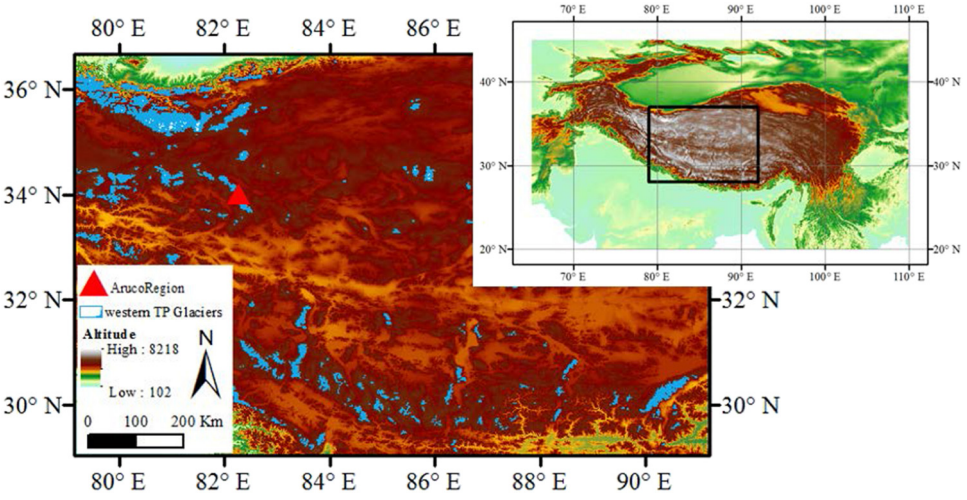

Figure 1: Map of extent of west Tibet (black line, longitude 79° to 92°E, and latitude 28° to 37°N) and distribution of glaciers (blue polygons, from the RGI 6.0) and location of the Aru region (red triangle).

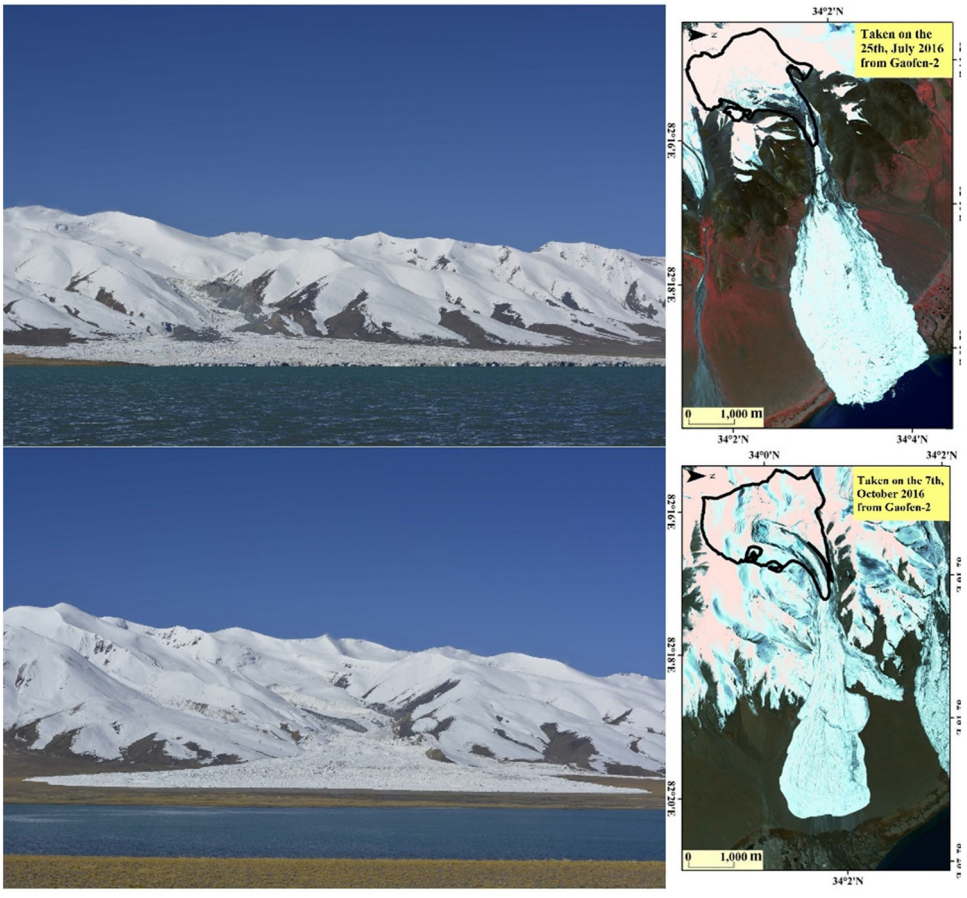

Figure 2: Scene photographs and remote-sensing images of Aru-1 and Aru-2. On the upper and lower left are the scene photographs of Aru-1 and Aru-2, respectively, taken on the opposite of the Aru Co on September 28, 2016 and on the right is the multispectral composite imaginary from Gaofen-2.

and precipitation enhancement over recent years in this region are supposed to have triggered the twin collapses. In addition, the glacier models and remote-sensing data play a crucial role in determining the dynamics and mechanisms of the twin collapses as they are located in the most remote region in the western Tibetan Plateau. A thermo-mechanical glacier model was utilized to simulate the polythermal structure for the twin glaciers, which provides infiltrating melt water to lubricate the ice/bed surface in the frontal zones and develops a progressively steepening geometry upstream of the cold-based fronts [10]. The thickness, velocities, basal shear stresses, and ice damage prior to the collapses based on the polythermal structure of the two glaciers were described exactly in detail in a subsequent study [11]. Long-term remote-sensing data from 1971 to 2016 demonstrate that the mass balance of two glaciers were negative before 1999 but turned to positive as a response to the increase in precipitation after 1999 [12]. Moreover, as the glacier collapses are a kind of gravitational mass flow, they can generate seismic signals. Therefore, seismic wave inversion was also applied on the glacier collapses to derive the motion parameters, including the mass and friction coefficient, to analyze the flow dynamics [13].

There are few studies that focus on the geometric features of the twin glaciers although the shape and size of the glaciers play a vital role in the dynamic process. The geometric features of glaciers are crucial inputs and important parameters to investigate the glacier dynamics, including the glacier centerline, longitudinal topography, and transverse profile. As the plane geometric feature of the glaciers, the centerline is capable of determining the change of glacier length, inferring the velocity field, estimating the ice volume, and developing the flowline model [14–17]. In this study, our main objectives are to find a method to distinguish the potentially collapsing glaciers from those other glaciers in the western Tibetan Plateau through the geometric features of glaciers and furthermore interpret the physical mechanisms contributing to the glacier collapses. When all the glaciers in the Aru Co basin, the Grand Aru Co (including several adjacent lakes to the Aru Co) basin, or even the western Tibetan Plateau are considered, it can be assumed that they are subject to the approximately same meteorological (precipitation and temperature), ice (density and viscosity), and geological (lithology and structure) conditions. The western Tibetan Plateau is distinctly located in the westerly domain, where the westerlies and continental climatic conditions play a dominant role [18]. What makes the twin glacier collapse abnormal in the western Tibetan Plateau can be acquired from their similarities between each other and their differences from other glaciers. The glacier morphology represents one of the important basic conditions, resulting in the twin collapses [10]. The curved shape in planform geometry of the two glacier is believed to influence the stability of the two glaciers by causing lateral and horizontal resistance [19].

In our study, the geometric features of the glaciers are derived from the centerlines and the degree of geometric similarity among the glaciers in the Aru Co, the Grand Aru Co, and the western Tibetan Plateau is determined quantitatively by a mathematical method [20]. Therefore, the degree of similarity to the target glaciers (Aru-1 and Aru-2) can be viewed as an index to assess the risk of glacier collapse in the study areas. Inspired by the geometry and morphology of meandering river channels [21], our study simulates the energy distribution and compensation status in glacier reaches to investigate the mechanisms of the geometric features of the twin collapsed glaciers based upon the energy conservation.

2 Study area, data, and methods

2.1 Study area

The western Tibetan Plateau (Figure 1) is a remote area on the edge of the Himalayas on the Tibetan Plateau, between 29°N and 37°N in latitude and between 79°E and 91°E in longitude, which covers mostly northwestern Shigatse and Nagri Prefectures [22]. Results based on reanalysis data and climate models indicate that precipitation in this region is increasing due to the strong water vapor transport from the dominant midlatitude westerlies [2]. Increasing evidence from satellite data and atmospheric reanalysis has shown a systematic increase in the warming rate with elevation in the western Tibetan Plateau [23]. In agreement with the general uptrend of precipitation and the enhanced warming with elevation, the glaciers in this region have experienced less retreat than the Himalayas [24] or even slightly advance [25]. In this study, all the glaciers (more than 20,000) in the western Tibetan Plateau were investigated of their risk of collapse.

Particularly, the twin glaciers (34.03°N; 82.25°E) collapsed in the Aru Co basin, Ngari Prefecture in the western Tibetan Plateau, where the elevation ranges between 5,250 and 6,150 m a.s.l., and the basin area is approximately 27 km^2 including no more than 30 glaciers. Aru-1 and Aru-2 are the two largest and longest glaciers among the glaciers from a glacier group in the Aru Co basin. The

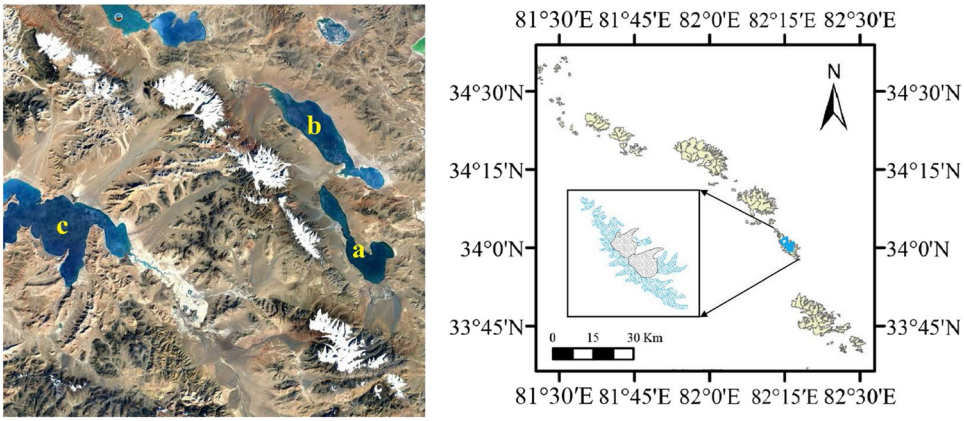

Figure 3: The extent of the Grand Aru Co basins, including the Aru Co (a), the Memar Co (b), and the Lumajiangdog Co (c) and several other small basins, and the outlines of all the glaciers in this region (the blue polygons are the Aru-1 and Aru-2, and the right interior rectangle covers the Aru Co basin with gray Aru-1 and Aru-2 outlines that had collapsed).

climatic and geographic conditions are believed to be fundamentally identical with all the glaciers in the Aru Co basin. To expand the research on the dynamics and mechanism of glacier collapses, the study takes the adjacent basins into consideration, including the Aru Co, the Memar Co, the Lumajiangdong Co, and several other relatively smaller lake basins. The Grand Aru Co basins cover an area of 362.65 km^2 with 271 glaciers (Figure 3).

2.2 Data

In this study, glacier outlines and a digital elevation model (DEM) are required as input data (Table 1) to derive centerlines for each glacier in the western Tibetan Plateau [26]. The glacier outlines in the western Tibetan Plateau are retrieved from the RGI 6.0 (http://www.glims.org/RGI/). DEM data is also required to obtain the centerlines of each glacier. The DEM product used herein covering the study area of interest is extracted from the Advanced Spaceborne Thermal Emission and Reflection Radiometer Global Digital Elevation Model (ASTER GDEM) dataset of the Tibetan Plateau, downloaded from the National Tibetan Plateau/Third Pole Environment Data Center (https://data.tpdc.ac.cn/en).

Despite sparse observations over the western Tibetan Plateau, especially at the glacierized areas due to the severe weather, complex topography, and harsh environmental conditions, an automatic weather station (AWS) was established near the Aru-2 in Oct 2016 during the first field work there, and precipitation and temperature data were collected from the date of establishment until September 2019. The mean temperature there in the monsoon season (between July and September) is over the freezing point, and the highest value is 7.2°C in August. The recorded mean annual precipitation acquired from a T200B gauge reaches 333 mm, which is more than double that of at Nagri meteorological station [5]. The positive precipitation trend in the Aru Co basin agrees with the result of recent research across the Tibetan Plateau from climatic models and reanalysis data, which indicates that the spatial pattern in the western Tibetan Plateau is turning to increasingly wetter [2].

2.3 Methods

2.3.1 Deriving the glacier centerlines

The Open Global Glacier Model (OGGM) is a modular and open-source glacier model to consistently simulate past

Table 1: Data used in the study and their statistical characteristics

Data	Source	Statistical characteristics
DEM	ASTER GDEM	30 m spatial resolution and 1° × 1° tiles
Glacier centerlines	RGI 6.0	30 Glacier outlines in Aru Co region and 271 outlines in Grand Aru Co regions
Climate data	AWS	Precipitation and temperature data from Oct 2016 to Sep 2019

and future changes of any glacier, including data-downloading tools, a preprocessing module, a mass balance model, and an ice-flow model [27]. The release of OGGM benefits from recent advances in the global availability of data and methods on glacier modeling, especially a geometrical routing algorithm that can automatically identify the glacier centerlines [26].

The preprocessing and flow-line modules in OGGM are used to compute the glacier centerlines in this study. In the preprocessing part of the workflow, a layer composed of glacier outlines derived from the RGI 6.0 and the other layer of the corresponding DEM (here GDEM in the western Tibetan Plateau) are merged with each other. The step to derive the glacier centerlines based on the novel and robust algorithm of Kienholz et al. [26] is of great complexity. First, the glacier heads and termini, which connect the centerlines, are identified. Second, a least-cost approach is applied to determine and optimize the least-cost route, representing the glacier centerlines. The route cost C is defined by the total penalty values $\sum P$ in all the grid cells (10 m × 10 m) along the selected route connecting the glacier head and the terminus. The penalty value P_i for grid cell i, comprised of the Euclidean distance-induced and elevation-induced penalty value, can be obtained from the following equation:

$$P_i = \left(\frac{D_{\max} - D_i}{D_{\max}} \cdot f_1\right)^a + \left(\frac{Z_i - Z_{\min}}{Z_{\max} - Z_{\min}} \cdot f_2\right)^b, \quad (1)$$

where the first right term, $\left(\frac{D_{\max} - D_i}{D_{\max}} \cdot f_1\right)^a$, represents the Euclidean distance-induced penalty value, forcing the selected route to the glacier center, and the second right term, $\left(\frac{Z_i - Z_{\min}}{Z_{\max} - Z_{\min}} \cdot f_2\right)^b$, depicts the elevation-induced penalty value to make the route downslope. D_i, $D_{\max}$, and $D_{\min}$ separately stand for the Euclidean distance from cell to the nearest glacier boundary, the maximum and minimum Euclidean distance from any point to the glacier boundary. Similar to the Euclidean distance, Z_i, $Z_{\max}$, and $Z_{\min}$ are the elevation in cell i, the highest and lowest elevation in the glacier. The coefficients (f_1 and f_2) are the scale parameters, and the exponents (a and b) are the weights. Finally, the above least-cost route obtained in the second step is smoothed into the glacier centerline.

2.3.2 Computing the similarity between the centerlines of the target glaciers and other glaciers

To compute the similarities between the centerlines of the target glaciers (Aru-1 and Aru-2) and those of the other glaciers, a well-known and effective metric for measuring resemblance of polygonal curves is introduced in this study, in which the location and ordering of the discrete points along the curves are considered. This metric, called the Fréchet distance, was firstly released by Fréchet in 1906, and a dog-and-leash interpretation of this distance (Figure 4a) was intuitively demonstrated [28]. Suppose there are two curves (P and Q), with P a man walking a dog and Q the dog; both can vary their own walking velocities independently without backtracking.

The Fréchet distance reflects the length of the shortest leash that is long enough for traversing both curves. As the computation of the exact continuous Fréchet distance (δ_F) is greatly sophisticated by means of the parametric search technique, Eiter and Manila described a discrete Fréchet distance (δ_{dF}) to approximate δ_F based on the investigation of all the possible couplings between the endpoints of the line segments of the polygonal curves [20]. The mathematical definition of δ_{dF} between the polygonal curves P and Q (Figure 4b) can be presented as follows:

$$\delta_{dF}(P, Q) = \min_{i=1,\ldots,m} \max d(u_{a_i}, v_{b_i}), \quad (2)$$

where $d(u_{a_i}, v_{b_i})$ is the coupling distance between the distinct pairs (u_{a_i}, v_{b_i}) from $\sigma(P) \times \sigma(Q)$. $\sigma(P)$ and $\sigma(Q)$ represent the sequence of endpoints of the line segments of polygonal curves P and Q, that is,

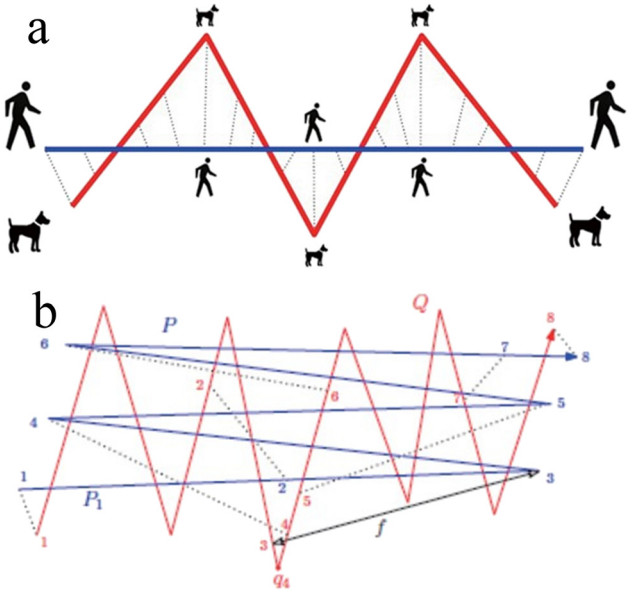

Figure 4: The simplified explanation (a) and the mathematical definition (b) of the Fréchet distance. The former explanation is based on the dog-and-leash interpretation. In the latter mathematical definition, the blue line is the P (a man walking a dog with a line) and the red line is the Q (the dog). The numbers denote the segments that link the points on P and Q.

$$\begin{aligned}\sigma(P) &= (u_1,\ldots,u_p),\\ \sigma(Q) &= (v_1,\ldots,v_q),\\ \sigma(P)\times\sigma(Q) &= (u_{a_1}, v_{b_1}), (u_{a_2}, v_{b_2}),\ldots,(u_{a_m}, v_{b_m}),\end{aligned} \tag{3}$$

where the subscript $(a_1, a_1,\ldots, a_m)$ is $(1, 2,..., p)$ and $(a_1, a_1, \ldots, a_m)$ is $(1, 2,..., q)$. For all subscripts $i = 1,\ldots, q$ in (u_{a_i}, v_{b_i}), there is a rule set as $a_{i+1} = a_i$ or $a_{i+1} = a_i + 1$, and $b_{i+1} = b_i$ or $b_{i+1} = b_i + 1$, which leads the couplings to comply with the order of the points in poly and poral curves P and Q. The maximum of the coupling distance $d(u_{a_i}, v_{b_i})$ forces the dog leash to be sufficient to link the curves, and then the minimum function optimizes the leash to be the shortest one. Due to a variety of applications of the discrete Fréchet distance in several fields, including computer vision, bioinformatics, computational geometry, and parametric curve approximations [29–32], this algorithm is deemed to be a reasonable method to quantitatively determine the resemblance between the glacier centerline of the Aru-1 or Aru-2 and that of the other glaciers in the study area. In the practical computation, a programming module coded with Python 3.7 based on the preceding algorithm has been applied in this study.

2.3.3 Understanding the meandering of the glacier centerlines

Few recent studies were reported to focus on the planform curvature of glacier centerlines, in spite of the fact that numerous mountain glaciers are tending to take longitudinal curving paths in valleys, with a wide range of degrees from gentle arcs to nearly perpendicular turns [33]. Nevertheless, during the early 1960s and the late 1980s, based on the detailed areal coverage of the velocity field and strain distribution on a small valley glacier with roughly constant curvature for much of its length, several glaciologists had quantitatively presented considerable methods and descriptions to interpret the asymmetric patterns of stress and velocity about the curving channel centerlines [34–37]. In a hypothetical curving glacier channel with the rectangular profile of uniform width, the longitudinal stress σ and velocity U can be obtained as follows:

$$\begin{aligned}\sigma(\xi) &= -\frac{1}{2} + \frac{\ln\xi_1}{(\xi_1^2-1)}\left(\frac{\xi_1}{\xi}\right)^2\\ U(\xi) &= -\xi\ln\xi + \xi\ln\xi\left[\frac{1-\xi^{-2}}{1-\xi_1^{-2}}\right],\end{aligned} \tag{4}$$

where the $\xi = r/R_0$ is a nondimension variable while the $\xi_1 = R_0/R_1$ is a dimensionless parameter, in which r, R_0, and R_1 are the radial distance from the center of the curvature, the minimum radius, and maximum radius, respectively, in cylindrical coordinates [38]. As seen in equation (4), both the longitudinal shear stress and velocity are asymmetric around the glacier channel centerline, which facilitates the understanding of the glacier centerline meandering and glacier collapsing.

Moreover, the energy compensation theory of a meandering river in a curving channel provides inspiration to explain the similar case of glacier flow in spite of the great difference in Reynolds and Froude numbers between the glacier and the river flow [39]. For a glacier segment in a relative equilibrium state, the mean energy during a specific time is presented as follows:

$$\bar{E}_i = \frac{1}{T}\int_0^T \gamma\Delta Z_i \mathrm{d}t + \frac{1}{T}\int_0^T \gamma\frac{U_i^2}{2g}\mathrm{d}t, \tag{5}$$

where the first right term is the potential energy and the second is the kinetic energy. When two cross sections, the upstream one in the straight channel and the downstream one in the bend, are considered, the longitudinal velocity, in other words the kinetic energy, decreases as the glacier flows due the equation (4) and the basal friction. Nonetheless, the curvature of the second cross section can result in an increase in the upstream ice depth, consequently increasing the potential energy, which compensates the dissipation of the kinetic energy in the channel reach. This conceptual procedure suggests that the curvature of the glacier channel is related to the kinetic energy loss. This relationship between the difference in kinetic energy between upstream and downstream cross sections and the channel curvature is explicitly given as follows:

$$\Delta E_k = \frac{1}{T}\int_0^T \frac{U_1^2(t)}{2g}\mathrm{d}t - \frac{1}{T}\int_0^T \frac{U_1^2(t)}{2g}\mathrm{d}t = \psi(\xi), \tag{6}$$

where the $\psi(\xi)$ states that the kinetic energy difference is a function of the shape factor ξ in the bend. Considering two extreme cases, a uniform straight channel and an orthogonal one with a right-angle turn, under the former case, the curvature along the entire glacier is zero, leading to a steady state of the glacier, that is, the velocity remains unchanged; whereas under the latter case, the velocity in the downstream cross section approaches zero and all the kinetic energy vanishes, in accordance with the infinite curvature.

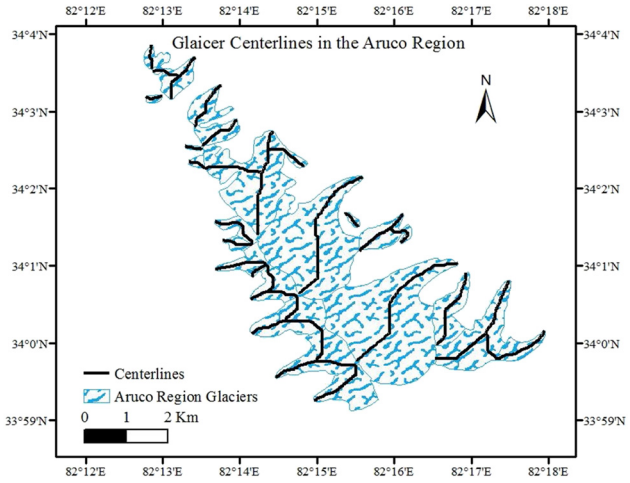

Figure 5: The glacier centerlines in the Aru Co regions.

3 Results

3.1 Glacier centerlines

First, the glacier centerlines in the Aru Co and the Grand Aru Co regions are derived by the least-cost approach in the preprocessing and flow-line modules of OGGM (Figures 5 and 6). In the Aru Co region, the centerlines of the Aru-1 and Aru-2 are the two longest (3.47 and 3.49 km) ones, in accordance with the area of these two glaciers (3.55 and 4.65 km^2). When all the 30 glaciers in the Aru Co region are divided into four classes by the area and the centerline length, Aru-1 and Aru-2 are in the same class as seen in Table 2, which illustrates that the glaciers in that class are prone to collapse as seen in Section 4.1. The Aru-1 and Aru-2 glaciers are the "vital few," which means that only twin collapsed glaciers in the Aru Co region account for the most area and centerline length of the glaciers [40]. The great loss of these twin glaciers has resulted in severe damage to the environment and solid water resource in the Aru Co region.

Table 2: Classification of the glaciers in the Aru Co region according to area and centerline length

Area (km^2)	Number of glaciers	Centerline length (km)	Number of glaciers
<1	24	<1	13
[1, 3)	4	[1, 3)	15
[3, 5)	2	[3, 5)	2
≥5	0	≥5	0

The massive differences in area and centerline length between the twin glaciers and the other glaciers in the Aru Co region make it that this region is not well grounded to find out the potential glaciers because of the insufficient glacier samples. To seek out the high-risk glaciers that are likely to collapse, we spread the study area to the Grand Aru Co region (Figure 6), which contains 271 glaciers. All the glaciers in the Grand Aru Co region are also divided into four classes by the area and centerline length as the same aforementioned standards as seen in Table 3. In this chart, there are dozens of glaciers in the same order of magnitude with Aru-1 and Aru-2. Therefore, the glacier samples are sufficient to compute the Fréchet distance between them and the target glaciers (Aru-1 and Aru-2). In the Grand Aru Co region, small glaciers (area <1 km^2 and centerline length <1 km) take up more than half, which are not considered in the analysis of Fréchet distance since these glaciers likely cannot collapse as Aru-1 and Aru-2 did.

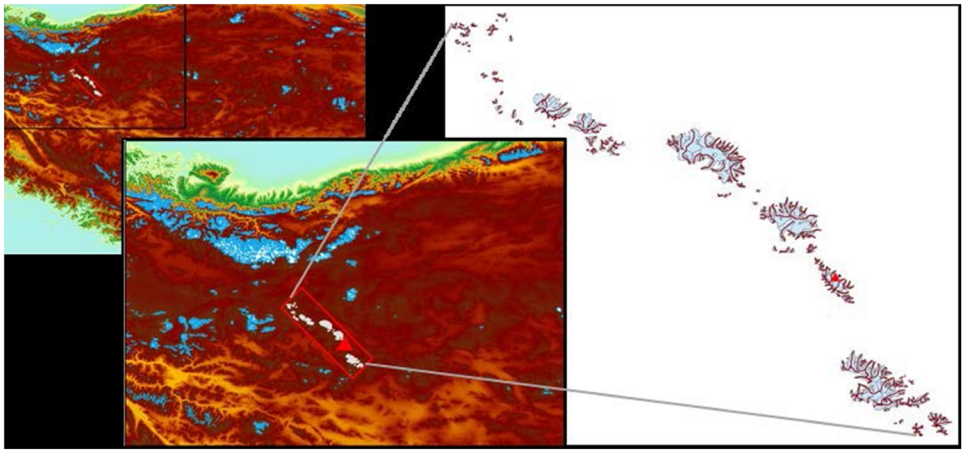

Figure 6: The glacier centerlines in the Grand Aru Co regions.

Table 3: Classification of the glaciers in the Grand Aru Co region according to area and centerline length

Area (km^2)	Number of glaciers	Centerline length (km)	Number of glaciers
<1	197	<1	158
[1, 3)	39	[1, 3)	71
[3, 5)	15	[3, 5)	29
≥5	20	≥5	13

3.2 Centerline similarity

To find a glacier centerline that is similar to the given ones (Aru-1 and Aru-2), the Fréchet distance, which used to match geometric patterns, is computed in the Aru Co region and the Grand Aru Co region. The lower the Fréchet distance is, the more similar the two glacier centerlines are to each other. The target glaciers are Aru-1 and Aru-2, and the Fréchet distance between the other glaciers and these two target glaciers in the Aru Co region and the Grand Aru Co region is listed in the following two charts (Tables 4 and 5). The $\mathcal{F}$ denotes the Fréchet distance between any two glacier centerlines.

It can be seen from Table 4 that the Fréchet distance between Aru-1 and Aru-2 is less than 1 km, the lowest among all the $\mathcal{F}$ distances in the Aru Co region, which indicates that there is a marked resemblance between these two glacier centerlines so that they collapsed in such a similar way within such a short period. The other glaciers in this region bear little resemblance to these twin glaciers according to the result of the Fréchet distances, which agrees to the quantitative relations between the twin glaciers and the other glaciers in the Aru Co region. Therefore, the standard of resemblance between the target glacier centerlines and the other glaciers can be served by the Fréchet distance, and the maximum standard is 1 km. Only a glacier, whose centerline conforms the required standard, the Fréchet distance of less than 1 km, can be viewed as a glacier with risk of collapse. With this standard, all the glaciers in the western Tibetan Plateau can be easily double tested with Aru-1 and Ar-2 to find out the glaciers with risk of collapse in the similar way to Aru-1 and Aru-2.

Table 4: The Fréchet distances between the target glacier centerlines (Aru-1 and Aru-2) and the other glacier centerlines in the Aru Co region

F (Aru-1, other glaciers) (km)	Number of glaciers	*F* (Aru-2, other glaciers) (km)	Number of glaciers
<1	2	<1	1
[1, 2)	4	[1, 2)	5
[2, 3)	8	[2, 3)	8
[3, 4)	13	[3, 4)	13
[4, 5)	2	[4, 5)	2
>5	0	>5	0

Table 5: The Fréchet distances between the target glacier centerlines (Aru-1 and Aru-2) and the other glacier centerlines in the Grand Aru Co region

$\mathcal{F}$ (Aru-1, other glaciers) (km)	Number of glaciers	$\mathcal{F}$ (Aru-2, other glaciers) (km)	Number of glaciers
<1	10	<1	11
[1, 2)	45	[1, 2)	39
[2, 3)	161	[2, 3)	154
[3, 4)	85	[3, 4)	98
[4, 5)	16	[4, 5)	15
>5	11	>5	11

In the Grand Aru Co region, there are dozens of glaciers, whose $\mathcal{F}$ to the Aru-1 and Aru-2 is less than 1 km, which means that their centerlines are similar to those of the target twin glaciers (Table 5). These high-risk glaciers are also in the equal magnitude of area and centerline length to the twin glaciers. All these glaciers can be viewed as high risk to collapse and need prompt monitoring. This is a quite efficient method to find out the glaciers, which have the potential to collapse in the similar way to the Aru-1 and Aru-2. In addition, these risky glaciers all follow a winding course like S-shape (Figure 7). This similar route to meander between the glaciers and some rivers helps discover the physical

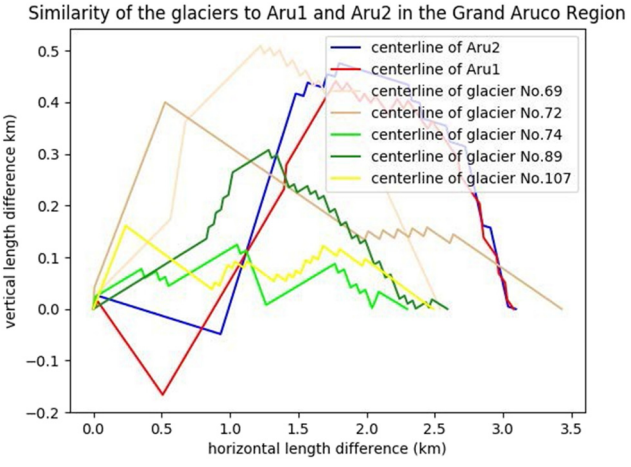

Figure 7: The similarity of glacier centerlines in the Grand Aru Co region and the *F* between all the glaciers herein and the target twin glaciers are less than 1 km.

mechanisms related to the glacier centerlines, which makes the glacier centerlines as a legitimate way to assess the risk to collapse in the west Tibet. The theoretical explanation based on the energy distribution along the centerlines is in Figure 8.

4 Discussions

4.1 Why the glaciers similar to Aru-1 and Aru-2 are prone to collapse?

On the one hand, Table 2 shows that there are no more glaciers in the same class of area and centerline length with the collapsed Aru-1 and Aru-2, indicating that the magnitude of other glaciers in Aru Co region is not sufficient to collapse. On the other hand, the lower Fréchet distances between the centerlines of Aru-1 and Aru-2 but higher among them with those of other glaciers also depict that the planform geometric features of the glaciers can be simply considered a quantitative indicator to distinguish the high-risk glaciers to collapse in the way of the twin glaciers. Therefore, it is convenient to make an assumption out of the beforementioned statistical analysis that the glaciers similar to Aru-1 and Aru-2 are prone to collapse.

The area and centerline length are both size features of the glaciers, which can be used to estimate the volume through a power law between the volume and area [41]. The size of Aru-1 and Aru-2 is close to each other, implying that only when the glaciers grow great enough can they collapse in the same way. The physical basis of this implication can be conveniently interpreted that the failure of the ice chunk in the sinuous valley glaciers requires sufficient potential gravity energy to transfer into the kinetic energy and then move downward into the alluvial fans with such a great velocity. This finding can be served as a complement to the results in the previous researches, which indicate that the twin collapses were triggered by the weather- and climate-driven external forcing [9]. Not only the external meteorological characteristics but also the internal features including geometric and thermal properties play significant roles in the dynamic process of the twin collapses.

For the present, on the basis of the field observation of the twin glaciers, there are several evidences to justify

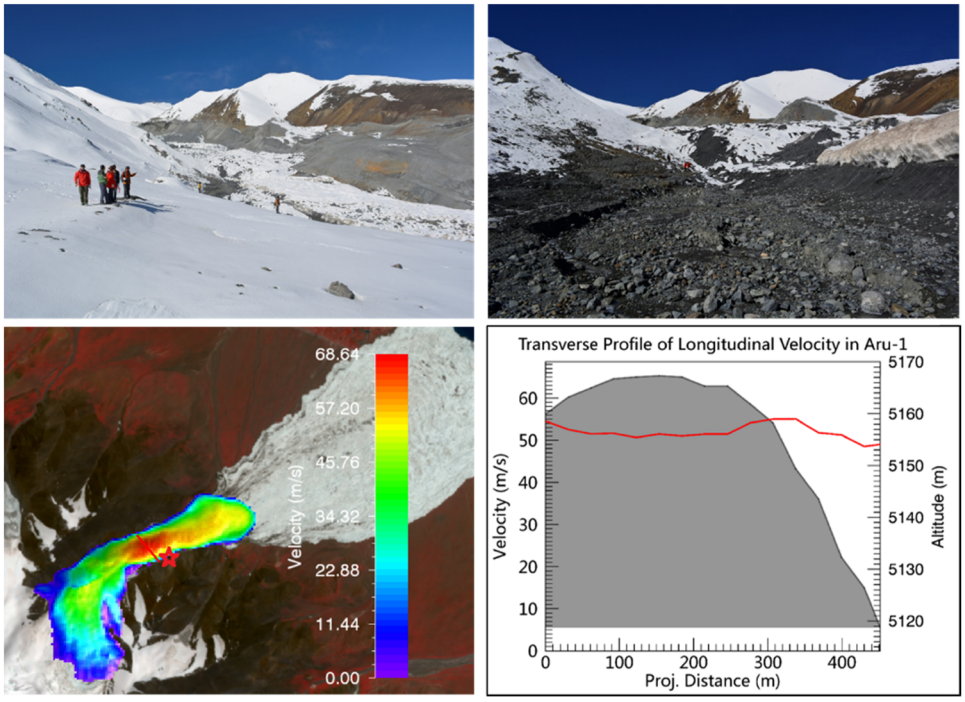

Figure 8: The upper two photos taken at the curvature (the red star in the lower left picture) in the postcollapse fieldwork of Aru-1 and the movement simulation result of Aru-1. In the upper two photos, the difference between the bilateral glacier sidewalls indicates that the collapsed ice chunks swept down the ice and debris on the opposite sidewall of the expedition but left the other undestroyed. The transverse profile of longitudinal velocity (the red line in the lower left picture), which is obtained from the simulation results of the postcollapse movement, verifies the asymmetric distribution of the velocity.

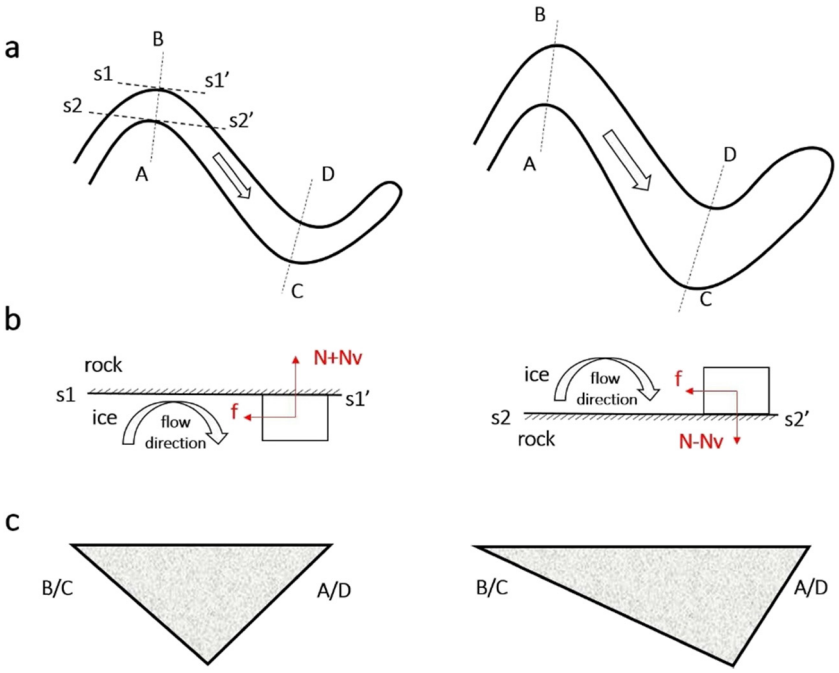

Figure 9: The physics of the glacier meandering. The section (a) indicates the marked differences of development of the glaciers between the two opposite longitudinal lateral sides in the curves, (b) implies the physical understanding of the mentioned differences, and (c) shows the variation of the vertical profiles in the curves.

the assumption that S-shape glaciers are prone to collapse. First, there are a considerable number of ice crevasses in the curvatures of the meandering glaciers because of the asymmetric velocity field of the transverse profile therein [10,42]. These crevasses break the "short-range" bond system of ice structure and then this widespread failure results in glacier collapse [43]. Second, the asymmetric movement traces (Figure 8) of the collapsed chunks on the bilateral valley sidewalls along the centerlines demonstrates that the ice chunks were rotating along the curvatures of the S-shape centerlines of the glaciers, which can be plainly verified by the kinetic simulation in the rapid mass movement model (Figure 8, the details of this simulation will be described in the coming study). Third, it can be simply and visually understood that the mid-segments of the S-shape glacier centerlines have the capability to bear sufficient stagnation of ice to collapse and then flow into the alluvial fans. Finally, the glacier is mathematically viewed as an array of vertical columns of unit cross-section area and varying height along the centerlines. The shape of the centerlines is originally controlled by the topography of the valley and then partly by the lateral friction between the ice and the viscosity, the development of which is still poorly understood. After a volume of literature reviews and several attempts, it is convincing to be very difficult to create a mathematically tractable model to simulate the glacier meandering, but the simulation work to obtain more conclusive evidences is still in progress and is expected to be published in the following study.

Additionally, an analytic description of energy distribution along the S-shape glacier centerlines is elucidated in Section 4.2, which provides a novel aspect to better understand this kind of rare phenomenon with geometric features of the glaciers.

4.2 The energy distribution along the glacier centerlines

According to the meandering patterns of the twin glaciers and the other high-risk glaciers, the glaciers with S-shape centerlines are prone to collapse in the way of Aru-1 and Aru-2. Initially, the erosion of the glacier forms the valley, and on the contrary, the development of glaciers is also shaped and constrained by the valleys [44]. The curvature of the two vertical sides along the centerlines has little difference to each other during the initial stage of the glaciation, whereas the difference is increasingly becoming higher and higher on the inside of the curves as the glacier develops (Figure 9a). This process can be

clarified by the microperspective of the change in the flow velocity inside of the curves (Figure 9b). The plane $S_1 - S_1'$ denotes the external side of the curves and the $S_2 - S_2'$ is the internal side. When the glacier flows through the curves, the velocity of the glacier section approaching has a normal component to enlarge the curvature of and flatten the vertical side of the valley (Figure 9c), whereas there is little change in the curvature of the plane. Figure 9c shows the change of the cross-sectional profile in curves, and more mass is left in the section between profiles A–B and C–D, which makes the glacier turn to be swollen with an unusually large ice volume within two curves.

The mechanism of glacier meandering is based on the principle of energy conservation, and the curvature of a glacier bend is controlled by the energy of ice flow, that is, the flow rate and the ice bed slope. Glacier meandering is a natural fluvial process to compensate for the energy loss so that the glacier could keep itself moving forward. The meandering centerlines of glaciers can result in a rise of ice thickness in the accumulation area, consequently increasing the potential energy in the route and leading to a rising in the slope of the ablation area as well as the kinetic energy increases. The latter, in turn, this rise in the slope and the kinetic energy, can result in a relative equilibrium state between the ice flow and the sediment transport in the glacier centerlines. The mechanism of glacier meandering may thus be rephrased as a glacier automatic regulating process. The degree of curvature in a channel reach is subject to the gained kinetic energy, that is, the difference in kinetic energy between upstream and downstream cross sections determines the degree of glacier meandering, which are in agreement with equation (6). The automatic kinetic energy compensation in glacier reaches could be used as the mechanism to explain glacier meandering. Such a mechanism can be justified by the field observation and numerical simulation in the forthcoming studies.

4.3 Why this kind of glacier collapse is hard to predict?

In this study, the method of the geometric similarity between the glaciers and the target glaciers is used to assess the risk of the glacier collapse. Nonetheless, this kind of glacier collapse is still hard to predict.

Although there are more than two hundred thousand mountain glaciers in the world, there are only dozens of glacier collapses reported and recorded [45,46]. The unstable steady equilibrium state of the glacier stays long term, while the glacier collapse is short lived and rarely recorded completely. The problem that there are extremely insufficient research objects makes many aspects of this kind of catastrophe remain obscure.

Additionally, the mechanism of the Aru-1 and Aru-2 glacier collapses is still a puzzle to the glaciologists. After the twin collapse, various mechanisms have been proposed to explain how they initiated, triggered, and developed, but our understanding remains incomplete [47]. The poly-thermal and soft-bed glacier features led to a progressive destabilization of the twin glaciers [11]. A hypothesis combined with thermal and hydrological control can partly demonstrate the glacier collapse. In the twin glacier collapse in Aru Co region, the temperature and crevasses affect supraglacial, englacial, and subglacial water to form vigorous hydrosystem in the whole glaciers. The englacial water is trapped in pores between the glacier and bedrocks in super-pressure state; therefore, any external process, such as an earthquake, an excess of water input from surface precipitation, or even a change in the englacial water level, can tip this delicate balance and release the pressure on the trapped water, making the water flow underneath the glacier and lubricating the ice bed. This kind of glacier collapse can be defined as a water-driven glacier collapse and extremely difficult to observe and obtain the englacial hydro-system in the glacier.

Lack of research objects and difficulty in observation limit the research on the glacier collapse and lead this kind of glacier hazard hard to predict. From this perspective, the geometric features of glaciers including the curvature of the centerlines are a rather simple but useful method to assess the potential glaciers that are prone to collapse.

5 Conclusion and future plan

In this study, the striking geometric similarity between the twin glaciers in Aru Co region is quantitatively interpreted by the magnitude and the Fréchet distance among the glacier centerlines in the Aru Co region and also in the Grand Aru Co region, which unearth some novel mechanisms of these terrible catastrophes in the western Tibetan Plateau [48,49]. In Aru Co region, the length of the centerlines and the area of Aru-1 and Aru-2 have similar resultant values, and also, the Fréchet distance between their centerlines is the lowest, which demonstrates that only when glaciers develop to the specific magnitude and

sinuous planform shape, can they collapse as the way of Aru-1 and Aru-2. In addition, the results of the magnitude and geometric similarity between the glacier centerlines in the Grand Aru Co region help filter a dozen of high-risky glaciers that need prompt observing and monitoring. Warning for glacier collapse is a huge challenge, and it is not feasible to focus on all the glaciers in the western Tibetan Plateau. Therefore, the practical significance of this study lies in selecting the glaciers, which are prone to collapse in the way of Aru-1 and Aru-2, on the basis of the geometric similarity of glaciers. Whereas the results in this study are generated from the twin glacier collapse, the approach has limitations of application to different kinds of glacier hazards including the surges of hanging glaciers and debris flow. Moreover, the length, area, and planform shape of glaciers are a part of the geometric features, which is not enough to present a comprehensive reflection of the glacier physics.

In a nutshell, this study provides a statement of a new perspective along with a few quantitatively statistical descriptions on the interactions between the planform shape of glaciers and the mechanism of the twin collapses. It is believed that these complex dynamics are directly generated by energy redistribution by simple causative mechanisms, which bear a strong resemblance to the meandering of rivers. In light of the similarities of the planform S-shape and the magnitude of the centerlines of the twin glaciers, more studies on the dynamics of the glacier collapses are called for. One study we plan to perform on these twin glacier collapses is to simulate the longitudinal velocity field of the sinuous glaciers during the movement processes and concentrate on its evolution in the glacier bends. Additionally, other geometric features of the glaciers including the curvature of the longitudinal profiles can be taken into consideration to investigate the glacier collapse.

Acknowledgments: We are grateful to data providers NASA ASTER and GLIMS science teams for the DEM and RGI 6.0. We also acknowledge support from the OGGM model. In addition, the authors thank the editors and four anonymous reviewers for their pertinent suggestions.

Funding information: This research has been financial supported by the Strategic Priority Research Program of the Chinese Academy of Sciences (grant no. XDA2006020102), the Second Tibetan Plateau Scientific Expedition and Research Program (grant no. 2019QZKK0201).

Author contributions: Both the authors contributed equally to this study.

Conflict of interest: The authors declare that they have no conflict of interest.

Data availability statement: The data used to support the findings of this study are available from the corresponding author upon request.

References

[1] Gasse F, Arnold M, Fontes JC, Fort M, Gibert E, Huc A, et al. A 13,000-year climate record from western Tibet. Nature. 1991 Oct;353(6346):742–5. doi: 10.1038/353742a0.

[2] RGI Consortium. Randolph Glacier Inventory – A Dataset of Global Glacier Outlines: Version 6.0: Technical Report, Global Land Ice Measurements from Space, Colorado, USA. Digital Media. 2017. doi: 10.7265/N5-RGI-60.

[3] Li D, Yang K, Tang W, Li X, Zhou X, Guo D. Characterizing precipitation in high altitudes of the western Tibetan plateau with a focus on major glacier areas. Int J Climatol. 2020 Oct;40(12):5114–27. doi: 10.1002/joc.6509.

[4] Qiu J. Giant, deadly ice slide baffles researchers. Nature. 2016. doi: 10.1038/nature.2016.20471.

[5] Tian L, Yao T, Gao Y, Thompson L, Mosley-Thompson E, Muhammad S, et al. Two glaciers collapse in western Tibet. J Glaciology. 2017 Feb;63(237):194–7. doi: 10.1017/jog.2016.122.

[6] Lei Y, Yao T, Tian L, Sheng Y, Liao J, Zhao H, et al. Response of downstream lakes to Aru glacier collapses on the western Tibetan Plateau. Cryosphere. 2021;15(1):199–214. doi: 10.5194/tc-15-199-2021.

[7] Yasuda T, Furuya M. Dynamics of surge-type glaciers in West Kunlun Shan, Northwestern Tibet. J Geophys Research: Earth Surf. 2015 Nov;120(11):2393–405. doi: 10.1002/2015JF003511.

[8] Thompson LG. Past, present, and future of glacier archives from the world's highest mountains. Proc Am Philos Soc. 2017;161(3):226–43.

[9] Qiu J. Ice on the run. Science. 2017 Dec;358(6367):1120–3. doi: 10.1126/science.358.6367.1120.

[10] Kääb A, Leinss S, Gilbert A, Bühler Y, Gascoin S, Evans SG, et al. Massive collapse of two glaciers in western Tibet in 2016 after surge-like instability. Nat Geosci. 2018 Feb;11(2):114–20. doi: 10.1126/10.1038/s41561-017-0039-7.

[11] Gilbert A, Leinss S, Kargel J, Kääb A, Gascoin S, Leonard G, et al. Mechanisms leading to the 2016 giant twin glacier collapses, Aru Range, Tibet. Cryosphere. 2018 Sep;12(9):2883–900. doi: 10.5194/tc-12-2883-2018.

[12] Zhang Z, Liu S, Zhang Y, Wei J, Jiang Z, Wu K. Glacier variations at Aru Co in western Tibet from 1971 to 2016 derived from remote-sensing data. J Glaciology. 2018 Jun;64(245):397–406. doi: 10.1017/jog.2018.34.

[13] Bai X, He S. Dynamic process of the massive Aru glacier collapse in Tibet. Landslides. 2020 Jun;17(6):1353–61. doi: 10.1007/s10346-019-01337-x.

[14] Zhang D, Yao X, Duan H, Liu S, Guo W, Sun M, et al. A new automatic approach for extracting glacier centerlines based on

Euclidean allocation. Cryosphere. 2021;15(4):1955–73. doi: 10.5194/tc-15-1955-2021.
[15] Nuth C, Kohler J, König M, Von Deschwanden A, Hagen JO, Kääb A, et al. Decadal changes from a multi-temporal glacier inventory of Svalbard. Cryosphere. 2013;7(5):1603–21. doi: 10.5194/tc-7-1603-2013.
[16] Oerlemans J. A flowline model for Nigardsbreen, Norway: projection of future glacier length based on dynamic calibration with the historic record. Ann Glaciology. 1997;24:382–9. doi: 10.3189/S0260305500012489.
[17] Linsbauer A, Paul F, Haeberli W. Modeling glacier thickness distribution and bed topography over entire mountain ranges with GlabTop: application of a fast and robust approach. J Geophys Research: Earth Surf. 2012;117(F3). doi: 10.1029/2011JF002313.
[18] Yao T, Masson-Delmotte V, Gao J, Yu W, Yang X, Risi C, et al. A review of climatic controls on delta O^{18} in precipitation over the Tibetan Plateau: observations and simulations. Rev Geophysics. 2013 Dec;51(4):525–48. doi: 10.1002/rog.20023.
[19] Haeberli W, Colin AW, John FS. Snow and ice-related hazards, risks, and disasters. Waltham, MA: Academic Press; 2014.
[20] Eiter T, Mannila H. Computing discrete Fréchet distance. Technical Report CD-TR 94/64. TU Vienna, Austria: Christian Doppler Laboratory for Expert Systems; 1994.
[21] Zeller J. Meandering channels in Switzerland. Int Assoc Sci Hydrol Publ. 1967;75:174–86.
[22] Razi AS, Levin V, Roecker SW, Huang GcD. Crustal and uppermost mantle structure beneath western Tibetan Plateau using seismic travel time tomography. Geochem Geophys Geosyst. 2014 Feb;15(2):434–52. doi: 10.1002/2013GC005143.
[23] Mountain Research Initiative EDW Working Group. Elevation-dependent warming in mountain regions of the world. Nature Climate Change. 2015 May;5(5):424–30. doi: 10.1038/nclimate2563.
[24] Bolch T, Kulkarni A, Kaab A, Huggel C, Paul F, Cogley JG, et al. The state and fate of Himalayan glaciers. Science. 2012 Apr;336(6079):310–4. doi: 10.1126/science.1215828.
[25] Yao T, Thompson L, Yang W, Yu W, Gao Y, Guo X, et al. Different glacier status with atmospheric circulations in Tibetan Plateau and surroundings. Nat Clim Change. 2012 Sep;2(9):663–7. doi: 10.1038/nclimate1580.
[26] Kienholz C, Rich JL, Arendt AA, Hock R. A new method for deriving glacier centerlines applied to glaciers in Alaska and northwest Canada. Cryosphere. 2014 Mar;8(2):503–19. doi: 10.5194/tc-8-503-2014.
[27] Maussion F, Butenko A, Champollion N, Dusch M, Eis J, Fourteau K, et al. The open global glacier model (OGGM) v1.1. Geosci Model Dev. 2019 Mar;12(3):909–31. doi: 10.5194/gmd-12-909-2019.
[28] Fréchet MM. Sur quelques points du calcul fonctionnel. Rendiconti del Circolo Matem- atico di Palermo (1884–1940). 1906;22(1):1–72.
[29] Alt H, Knauer C, Wenk C. Matching polygonal curves with respect to the Fréchet distance. In: Goos G, Hartmanis J, van Leeuwen J, Ferreira A, Reichel H, editors. Annual Symposium on Theoretical Aspects of Computer Science. Berlin, Heidelberg: Springer; 2001. p. 63–74.
[30] Wenk C. Shape matching in higher dimensions. PhD thesis. Berlin: Freie Universität; 2003.
[31] Jekel CF, Venter G, Venter MP, Stander N, Haftka RT. Similarity measures for identifying material parameters from hysteresis loops using inverse analysis. Int J Mater Form. 2019 May;12(3):355–78. doi: 10.1007/s12289-018-1421-8.
[32] Yu P, Xie W, Liu LX, Powell MS. Applying Fréchet distance to evaluate the discrepancy of product size distribution between single particle and monolayer multi-particle breakage. Powder Technol. 2019 Feb;344:647–53. doi: 10.1016/j.powtec.2018.12.043.
[33] Coffey KM, Paterson WSB. The Physics of Glaciers. Burlington: Elsevier Science; 2010.
[34] Allen CR, Kamba WB, Meier MF, Sharp RP. Structure of the lower blue glacier, Washington. J Geol. 1960 Nov;68(6):601–25. doi: 10.1086/626700.
[35] Meier MF, Barclay Kamba W, Allen CR, Sharp RP. Flow of blue glacier, olympic mountains, Washington, U.S.A. J Glaciol. 1974;13(68):187–212. doi: 10.3189/S0022143000023029.
[36] Echelmeyer KA. Response of blue glacier to a perturbation in ice thickness: theory and observation. PhD thesis. Pasadena, USA: California Institute of Technology; 1983.
[37] Echelmeyer K, Barclay K. Glacier flow in a curving channel. J Glaciology. 1987;33(115):281–92. doi: 10.3189/S0022143000008856.
[38] Nye JF. The mechanics of glacier flow. J Glaciology. 1952;2(12):82–93. doi: 10.3189/S0022143000033967.
[39] Chang HH. Minimum stream power and river channel patterns. J Hydrol. 1979 May;41(3–4):303–27. doi: 10.1016/0022-1694(79)90068-4.
[40] Liu C, Wang C, Zhang Zh, Zheng L. Scheduling with job-splitting considering learning and the vital-few laws. Comput Oper Res. 2018 Feb;90:264–74. doi: 10.1016/j.cor.2017.02.011.
[41] Bahr DB. Width and length scaling of glaciers. J Glaciology. 1997;43(145):557–62. doi: 10.3189/S0022143000035164.
[42] Cuffey KM, Paterson WSB. The physics of glaciers. 4th edn. Burlington, MA: Butterworth-Heinemann/Elsevier; 2010.
[43] Smalley I, Ng'ambi S. Problems with collapsible soils: particle types and inter-particle bonding. Open Geosci. 2019;11(1):829–36. doi: 10.1515/geo-2019-0064.
[44] Monkhouse FJ. Principles of physical geography. Washington: Rowman & Littlefield; 1964.
[45] Emmer A, Cook SJ, Frey H, Shugar DH. Geohazards and risks in high mountain regions. Front Earth Sci. 2021;9:754260. doi: 10.3389/feart.2021.754260.
[46] Truffer M, Kääb A, Harrison WD, Osipova GB, Nosenko GA, Espizua L, et al. Glacier surges. In: Haeberli W, Whiteman C, editors. Snow and ice-related hazards, risks, and disasters. 2nd ed. Amsterdam: Elsevier; 2021. p. 417–66. doi: 10.1016/B978-0-12-817129-5.00003-2.
[47] Farinotti D, Immerzeel WW, de Kok RJ, Quincey DJ, Dehecq A. Manifestations and mechanisms of the Karakoram glacier anomaly. 2020;13(1):8–16. doi: 10.1038/s41561-019-0513-5.
[48] Xiao L, Zhang Y, Ge T, Wang C, Wei M. Analysis, assessment and early warning of mudflow disasters along the shigatse section of the China–Nepal highway. Open Geosci. 2020;12(1):44–58. doi: 10.1515/geo-2020-0004.
[49] Wu C, Guo Y, Su L. Risk assessment of geological disasters in Nyingchi, Tibet. Open Geosci. 2021;13(1):219–32. doi: 10.1515/geo-2020-0208.